CHALMERS
UNIVERSITY OF TECHNOLOGY

Interface Layers of Niobium Nitride Thin Films

Downloaded from: https://research.chalmers.se, 2021-08-31 17:12 UTC

Citation for the original published paper (version of record):
Lubenschenko, A., Iachuk, V., Krause, S. et al (2019)
Interface Layers of Niobium Nitride Thin Films
Journal of Physics: Conference Series, 1410(1)
http://dx.doi.org/10.1088/1742-6596/1410/1/012124

N.B. When citing this work, cite the original published paper.

research.chalmers.se offers the possibility of retrieving research publications produced at Chalmers University of Technology.
It covers all kind of research output: articles, dissertations, conference papers, reports etc. since 2004.
research.chalmers.se is administrated and maintained by Chalmers Library

(article starts on next page)

Interface Layers of Niobium Nitride Thin Films

A V Lubenchenko[1], V A Iachuk[1], S Krause[2], A B Pavolotsky[2], D A Ivanov[1], O I Lubenchenko[1] and O N Pavlov[1]

[1]National Research University "Moscow Power Engineering Institute", Moscow, 111250, Russia

[2]Chalmers University of Technology, Göteborg, 41296, Sweden

Abstract. Intermediate layers formed by thin NbN films are studied. A surface phase of NbN different from the bulk one under the oxide layer and a layer consisting of NbN_x-SiO_y between the film and the substrate are found.

1. Introduction

Thin films of niobium nitride are widely used in hot electron bolometer mixers (HEB) which are the most sensitive detectors for spectroscopy in the terahertz frequency range above ca. 1 THz [1]. Performance of HEB's depends on uniformity of the 3-6 nm thin NbN layer [2]. It was found [3] that by air oxidation of NbN films a transition layer between niobium nitride and oxide is generated, about few monolayers thick. However, its phase compound was not clear. One of the purposes of this work is a study of this intermediate layer for films of different thicknesses. Operation properties of films depend on this interface significantly. Another purpose is to investigate the lower interface, between the NbN film and the substrate.

2. Experimental Details

NbN films were deposited on a silicon substrate by the method of magnetron sputtering in the experimental setting AJA Orion-5-U-D. The film thickness during sputtering was controlled by the known sputtering rate (the sputtering rate was approved by investigation of the films by TEM).

XPS spectra were recorded with the Nanofab 25 (NT-MDT) electron-ion spectroscopy platform. The pressure in the analysis chamber was of 10^{-7} Pa provided by the titanium sublimation pump and the ion pump. The residual pressure and composition of residual gas were monitored by a Bayard-Alpert vacuum gauge and a secondary ion mass-spectrometer. For XPS analysis, the X-ray source SPECS XR 50 with a dual Al/Mg anode was used providing 1486.6 eV and 1253.6 eV photons. The X-ray source was located at the angle of 54.7° relative to the analyzer axis. The spectra were recorded with the electrostatic hemispherical energy analyzer SPECS Phoibos 225. The energy resolution estimated as the full width at half maximum (FWHM) of the spectrometer at the Ag3d5/2 line (peak) was of 0.78 eV for non-monochromatic X-radiation Mg Kα. The energy positions of the spectra were calibrated with reference to the Cu2p3/2 (binding energy 932.62 eV), Ag3d5/2 (368.21 eV) and Au4f7/2 (83.95 eV) peaks. All sur-vey spectra scans were taken at a pass energy of 80 eV. The detailed scans of high intensity lines were in most cases recorded as wide as needed just to encompass the peak(s) of interest and were obtained with the pass energy of 20 eV. The energy analyzer was operated in Fixed Analyzer Transmission (FAT) mode.

The ion source SPECSIQE 12/38 was used for sputtering the samples. The ion source had differential pumping and was fed with 99.9995% pure Ar. The ion beam scanned the area of 2.8 mm × 4.0 mm at

Content from this work may be used under the terms of the Creative Commons Attribution 3.0 licence. Any further distribution of this work must maintain attribution to the author(s) and the title of the work, journal citation and DOI.
Published under licence by IOP Publishing Ltd

the incidence angle of 70° to the surface normal, the ion beam energy was of 1 keV. Ion profiling included total 5 cycles of sputtering with recording of XPS spectra before sputtering and after each cycle. For sputtering cycles #1–#5, each cycle was 20 min long.

3. Depth profiling

One of none-destructive methods of thin and ultra-thin films analysis is X-ray photoelectron spectroscopy (XPS). With the help of XPS chemical and phase depth profiling of surface is performed. By the standard XPS method, relative atomic concentrations are calculated assuming a homogeneous target by all the depth of profiling. However, real surfaces are always inhomogeneous and multicomponent by depth. Disregarding this leads to significant errors and depreciates information about relative atomic concentrations.

As a rule, a surficial region is not only multilayer but multicomponent and multiphase. Depth profiling based on interpretation of photoelectron spectra from such targets is a complex inverse problem with many a priori unknown parameters. For correct solution of this problem paper [4] offers: 1) a method of background subtraction considering the difference of energy losses on surface and in bulk; 2) using constant parameters in all the range of the photoelectron spectrum for background and line profile calculation; 3) using of line profile parameters from the spectra of Handbook of X-Ray Photoelectron Spectroscopy [5] for pure homogeneous targets; 4) simultaneous interpretation of different lines of the same element using the same model.

The reconstruction method of layer-by-layer profile is based on a target model that results from the history of its production and life. The principle statements of the target model used in this paper:

1) The target consists of few plane layers on a substrate. Each layer is homogeneous and may be multicomponent. Such statement is reasonable because an XPS signal is recorded from a surface area which dimensions are by orders greater than the probing depth. This area depends on focusing of the energy analyzed and geometry of the experiment and it is about 0.1 mm^2. The probing depth is about 10 nm. So the signal will be measurement area-averaged.

2) Inhomogeneities (islets, interlayer asperities, inclusions, etc.) are layer-averaged. Inhomogeneity rate will define relative concentrations of element phases.

3) After unload from the chamber, the surface is oxidized and oxide and suboxide layers are generated. As far as oxidation progresses from the surface, the oxidation level decreases with depth. Besides that, at the top a hydrocarbon layer will be precipitated.

To decrease the uncertainty of number of layers, we propose to introduce the minimum homogeneous layer thickness equal to the mean distance between monolayers in solid (0.5 nm). Let start the calculation from the maximum possible number of layers assuming each layer be of the constant oxidation rate. If calculation results that thickness of a layer be less than the minimum one, this layer is added to the next one with a higher oxidation rate of the main element. The newly formed layer will be multicomponent. This layer can be regarded as an inhomogeneous one averaged to a homogeneous layer of some effective thickness. The inhomogeneity degree may be estimated with the help of relative atomic concentration of the element in this layer. After that the layer thicknesses are recalculated. Such approach enables to decrease the number of alternate calculations significantly and to regard the alternates as profiles calculated with different depth detailing.

Layer thicknesses will be calculated by the formula [4]:

$$d_i = \lambda_i \cos\theta \ln\left(\frac{I_i/(n_i\omega_i(\gamma)\lambda_i)}{\sum_{j=0}^{i-1} I_j/(n_j\omega_j(\gamma)\lambda_j)} + 1\right) \quad (1)$$

where d_i is the thickness of the i-th layer, n is the atomic concentration, $\omega_i(\gamma)$ is the differential cross-section of photoelectron production [6], γ is the angle between the directions of incident radiation and to the energy analyzer, λ is the IMFP (IMFP is calculated by the TPP2M formula [7]), θ is the angle between the direction to the energy analyzer and the surface normal, I_i is the i-th peak intensity. The layers will be numerated upwards from the substrate. Number 0 means the substrate.

4. Results and Discussion

In this work, 5 nm film of NbN on a silicon substrate were studied. Standard XPS analysis of all samples identified presence of chemical elements like C, O, Nb, Si. Figure 1 shows survey spectra for a NbN 5 nm target after various stages of sputtering. Estimated relative atomic concentrations by XPS are presented in table 1.

Table 1. Relative atomic concentration.

	c, %					
	0	1	2	3	4	5
C	35.6	8.4	1.8			
O	33.0	30.3	18.6	40.4	14.4	16.0
N	6.1	15.6	24.2	12.8	26.0	21.0
Nb	23.1	42.8	48.4	41.3	45.3	29.5
Si	2.2	2.9	7.0	5.5	14.3	33.5

The XPS spectra can be used to analyze chemical bounds of elements and the chemical composition of the matter. For that an XPS line of a certain element is decomposed into corresponding peaks. Structure of these peaks may be quite complex due to chemical shift, satellite peaks, shift caused by sample charging etc. Additionally, shape and width of the peaks depend on various factors, and the peaks can over-lap. For deconvolution of XPS peaks, we used the method described in [8].

The shape of a spectral line of photoelectrons will be determined by a convolution of functions describing the natural line shape and instrumental broadening. The natural line shape will be described the Doniach-Šunjić expression and the instrumental broadening function by the Gauss function. We suggest to take the binding energy and spin-orbital interaction energy for chemically pure elements from the experimental data of the Handbook of X-ray Photoelectron Spectroscopy. The chemical shift energy is almost linearly proportional to the oxidation level, so it is enough to find the chemical shift energy for the most oxidized element. For example, we used a value of 5.31 eV for niobium oxide Nb_2O_5.

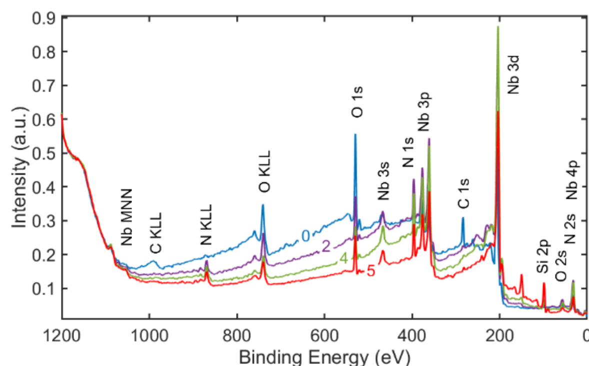

Figure 1. Survey XPS spectra. Target: NbN, 5 nm. Numbers: number of sputtering cycles.

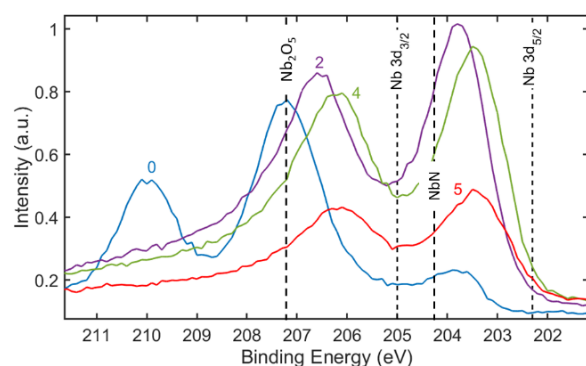

Figure 2. XPS spectra of line Nb 3d. Target: NbN, 5 nm. Numbers: number of sputtering cycles.

The chemical shift energy of nitrogen-niobium compound depends significantly on its stoichiometry. Paper [8] shows a dependence of chemical shift for lines Nb 3d and N 1s on the stoichiometric coefficient x in compound NbN_x. After sputtering positions of NbN peaks in line Nb 3d changes to lesser binding energies (see 'figure 2'). This indicates that the phase compound of a NbN film changes to lesser x in NbN_x.

The obtained XPS spectra are shown in figure 3-5. Circles show recorded detailed spectra, the solid lines: calculated using method [4], the dotted line: separate calculated peaks. Information on chemical and phase composition on the layers was obtained by the analysis of peaks produced by elastically scattered electrons.

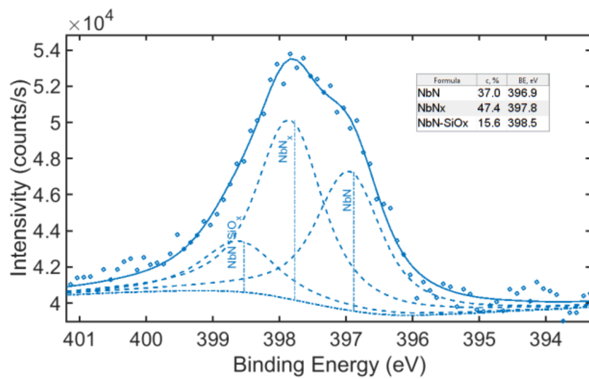

Figure 3. XPS spectra of line N 1s. Target: NbN, 5 nm. Solid lines: calculation. Circles: experimental data.

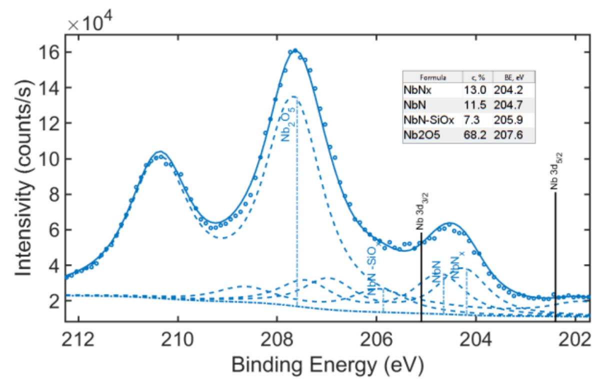

Figure 4. XPS spectra of line Nb 3d. Target: NbN, 5 nm. Solid lines: calculation. Circles: experimental data.

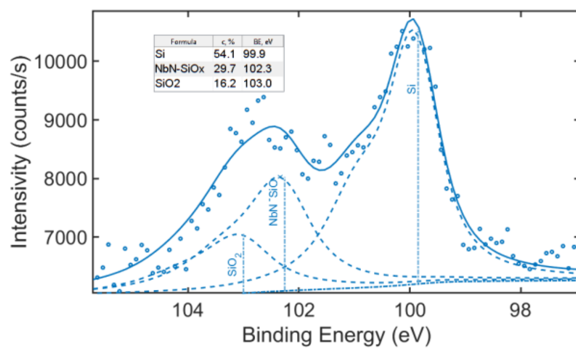

Figure 5. XPS spectra of line Si 2p. Target: NbN, 5 nm. Solid lines: calculation. Circles: experimental data.

As a result of this study, it was found that line N1s was decomposed into three peaks corresponding to two different phases of niobium nitride and complex compound of NbN_x and SiO_y ‘figure 3’. The peaks of these phases were observed in line Nb 3d ‘figure 4’ and line Si 2p ‘figure 5’. Following the data from [8] the phases of niobium nitride were determined: NbN и NbN_x, $x \approx 0.79$ that corresponded to Nb_5N_4. So before sputtering another phase was of lower oxidation rate of N. We assume these results show that by air oxidation under the oxide layer an intermediate layer is formed with a surface phase different from the phase of NbN in the bulk. The thickness of that layer is about one or two monolayers (1 nm). By sputtering of niobium nitride due to prevailing sputtering of nitrogen by argon ions (the sputtering yield of nitrogen is more than that of niobium) the phase of niobium nitride shifted to lesser x. After the 5th sputtering stage $x \approx 0.73$ that corresponded to Nb_4N_3.

Table 2. Chemical and Phase Depth Profiling of a $NbN/SiO_2/Si$ Target.

	d, nm		
	0	5	
6	0.8	-	hydrocarbons
5	2.9	-	Nb_2O_5
4	0.8	0.9	NbN_x
3	0.9	0.4	NbN
2	2.3	1.5	NbN_x-SiO_y
1	1.3	0.6	SiO_2
Substrate			Si

Interpretation of XPS spectra before and after sputtering enabled to determine thickness and phase compound of the transition layer between the NbN film and the substrate formed by film growth. Our

measurements showed the thickness of this layer about 0.5 nm. This layer consists of a complex compound of NbN_x and SiO_y. This conclusion results from decomposition of the line Si2p: it is decomposed into three doublets corresponding to Si, NbN_x-SiO_y and SiO_2 (see 'figures 3-5').
Table 2 displays computing results for thicknesses following the formula (1) from work which accounts for partial intensities obtained by decomposition of the lines N1s, Si2p and Nb3d.
Our investigation shows that the structure of NbN films is always complex, depending on conditions of growth and oxidation. Influence of interface onto HEB's performance requires further research.

References
[1] Meledin D, Pavolotsky A, Desmaris V et. all. 2009 *IEEE Transactions on Microwave Theory and Techniques* **57** 89–98.
[2] Sergeev A V and Reizer M Y 1996 *International Journal of Modern Physics B* **10** 635–67.
[3] Lubenchenko A V, Batrakov A A, Pavolotsky A B et. all. *EPJ Web of Conferences* vol 132, p 03053
[4] Lubenchenko A V, Batrakov A A, Pavolotsky A B, Lubenchenko O I and Ivanov D A 2018 *Applied Surface Science* **427** 711–21.
[5] Moulder J F, Stickle W F, Sobol P E and Bomben K D 1979 *Handbook of X Ray Photoelectron Spectroscopy: A Reference Book of Standard Spectra for Identification and Interpretation of XPS Data* (Physical Electronics).
[6] Yeh J J and Lindau I 1985 Atomic subshell photoionization cross sections and asymmetry parameters: $1 \leqslant Z \leqslant 103$ *Atomic Data and Nuclear Data Tables* **32** 1–155.
[7] Tanuma S, Powell C J and Penn D R 2003 *Surface and Interface Analysis* **35** 268–75.
[8] Prieto P, Galán L and Sanz J M 1991 *Surface Science* **251–252** 701–5.